Structural Durability & Health Monitoring

Tech Science Press

DOI: 10.32604/sdhm.2024.054761

ARTICLE

Construction Monitoring and Analysis of Asymmetric Prestressed Concrete Bridge Crossing Multiple-Line Railways

Yi Wang[1], Bing Wang[2], Changwen Li[2], Feng Zheng[1], Yong Liu[2] and Shaohua He[3,*]

[1]Guangzhou Railway Investment Construction Group Co., Ltd., Guangzhou, 510000, China

[2]China Railway Third Bureau Group Co., Ltd, Taiyuan, 030024, China

[3]School of Civil and Transportation Engineering, Guangdong University of Technology, Guangzhou, 510006, China

[*]Corresponding Author: Shaohua He. Email: hesh@gdut.edu.cn

Received: 06 June 2024 Accepted: 29 July 2024 Published: 15 January 2025

ABSTRACT

Complex bridge structures designed and constructed by humans often necessitate extensive on-site execution, which carries inherent risks. Consequently, a variety of engineering practices are employed to monitor bridge construction. This paper presents a case study of a large-span prestressed concrete (PC) variable-section continuous girder bridge in China, proposing a feedback system for construction monitoring and establishing a finite element (FE) analysis model for the entire bridge. The alignment of the completed bridge adheres to the initial design expectations, with maximum displacement and pre-arch differences from the ideal state measuring 6.39 and 17.7 mm, respectively, which were less than the 20 mm limit required by the specification. Additionally, the stress monitoring showed that the maximum compressive stress was 10.44 MPa, which was 7.5% different from the finite element results, and better predicted the most unfavorable possible location. These results demonstrate that a scientifically rigorous construction monitoring and feedback system can ensure the safety of bridge construction and meet the expected construction standards. The findings presented in this paper provide valuable insights for bridge construction monitoring practices.

KEYWORDS

Continuous girder bridge; construction monitoring; bridge alignment; stress monitoring

1 Introduction

In recent decades, large-span prestressed concrete (PC) variable-section continuous girder bridges have garnered significant attention in bridge construction due to their robust spanning capacity, elevated underbridge clearance, and seamless traffic flow [1–3]. The design and construction of these large-scale bridge structures rely heavily on human decision-making and financial investment. However, statistics indicate that more than 50% of accidents during the bridge construction phase involve girder bridges, with construction activities being the primary contributing factor [4]. Safety incidents during bridge construction not only result in significant economic losses but also endanger the safety of construction personnel. The occurrence of such accidents can be attributed to major causes, including unsafe conditions and unsafe behaviors [5]. However, the commitment to good practice by construction personnel and rigorous monitoring of the structure can significantly enhance construction safety [6].

Furthermore, numerous engineering cases highlight that the intricate design and construction of such complex structures entail considerable inherent risks, necessitating vigilant monitoring and proactive mitigation measures throughout the construction process [7–10].

Hence, increasing attention from scholars and engineers is directed towards monitoring bridge construction processes. For instance, Zasukhin et al. [11] underscored the importance of structural stress-strain monitoring during construction, citing several engineering cases. Such monitoring guides the construction process, offering timely feedback on structural conditions and mitigating operational emergencies, thereby enhancing structural safety and longevity. Li et al. [12] employed finite element (FE) methods to ensure smooth and secure construction, identifying critical risks through stress monitoring during bridge jacking procedures. Yin et al. [13] analyzed and discussed construction monitoring techniques for large-span V-structure tie arch bridges, emphasizing the need for both economic feasibility and scientific rigor. Inaudi et al. [14] utilized fiber optic deformation sensors to oversee railroad bridge construction, providing valuable insights for controlling construction processes and preventing structural cracking during bridge slippage. Zhang et al. [15] monitored the cable-stayed ropes force during the construction of a large-span cable-stayed bridge and analyzed the bridge alignment and main girder stresses. The results demonstrated that the measured values were in good agreement with the theoretical values, thereby providing greater assurance regarding the construction of the bridge. Similarly, Idriss [16] effectively monitored the construction of a high-performance PC highway bridge using buried sensors, systematically measuring material properties and prestress loss. Collectively, research and practical experiences demonstrate that construction monitoring is indispensable for ensuring the safe construction of bridges. By scrutinizing various aspects of structural development, construction monitoring identifies potential risks and corresponding mitigation strategies and guarantees the attainment of desired construction outcomes.

This paper focuses on the construction of a large-span PC variable-section continuous girder bridge in Guangzhou, China. The construction process of the bridge is divided into two stages: (a) the main girder construction stage and (b) the bridge rotation construction stage. Before the rotation construction stage, comprehensive construction monitoring was diligently conducted throughout the main girder construction stage to ensure the seamless advancement of the construction stage and adherence to design specifications. Construction control measures were implemented, including formwork elevation, bridge alignment, and structural stress management. A FE model was developed to compare with on-site measured data. A comprehensive construction monitoring feedback system was also proposed to guide the construction process and standardize the operation process of the construction personnel. Results indicate that the feedback system, rooted in scientific theory, effectively ensures that structural performance meets expected requirements, thus ensuring the smooth completion of the bridge. Moreover, the practices and monitoring systems implemented in this bridge construction serve as valuable references for future bridge construction monitoring endeavors.

2 Prototype Bridge Descriptions and Simulation Work

2.1 Prototype Bridge

The prototype SF/SG Ramp Bridge forms part of a railway bridge in Guangzhou, China. It constitutes a PC variable-section continuous girder bridge, necessitated by its traversal over multiple rail tracks, featuring a maximum longitudinal slope of 5.9% and a transverse slope of 2%. It is designed for a travel speed of 50 km/h and boasts a span distribution of 82.5 m + 82.5 m. As illustrated in Fig. 1, the bridge spans 165 m long, with a beam section height of 9 m at the pier and 3 m at the side span. The bottom of the box girder follows a parabolic curve, transitioning from 7 m at the pier center to the merging section. The cross-section comprises a box with five chambers, maintaining a standard width of 25 m. Construction material comprises C55 grade concrete, while the prestressing system employs a three-dimensional

tendon approach, utilizing high-strength-low-relaxation steel strands. These strands, boasting a nominal diameter of 15.2 mm and a standard strength of 1860 MPa, are deployed in the transverse, longitudinal, and vertical directions of the main girder.

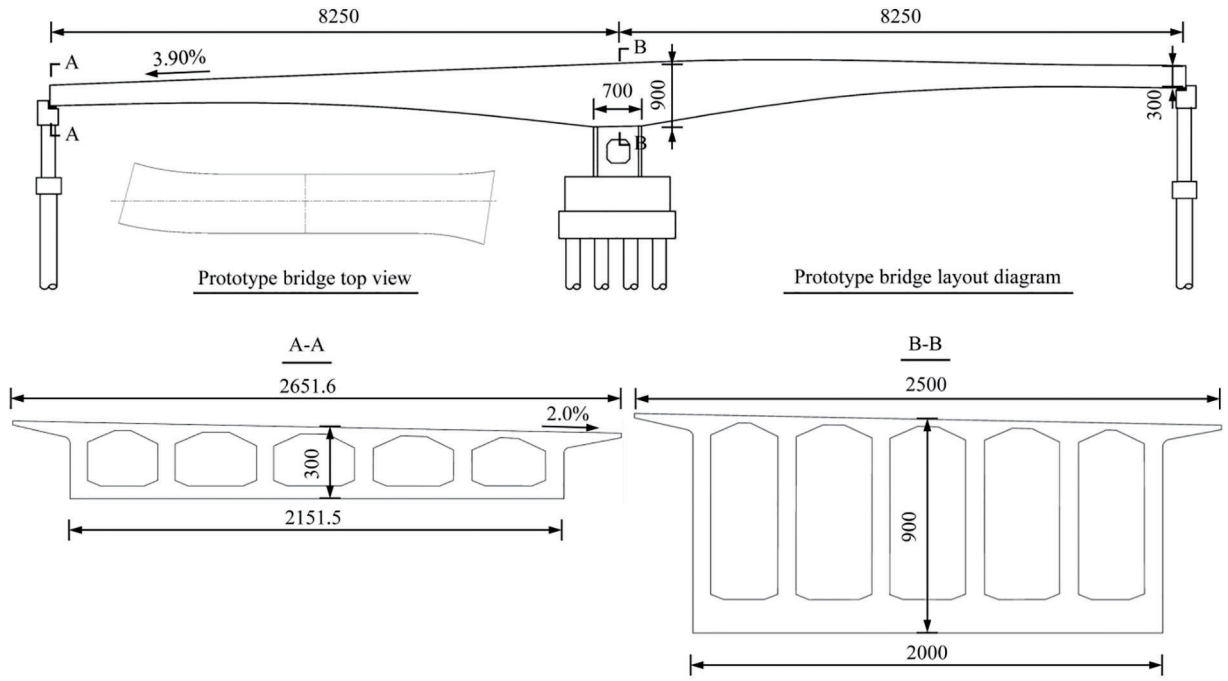

Figure 1: Configuration of the prototype bridge (unit: cm)

It is noteworthy to highlight that the main girder of the bridge comprises nine segments, all of which were fabricated at the specified location utilizing the full-support cast-in-place methodology. Each segment underwent a rigorous curing process lasting seven days, and subsequent prestressing was applied once its compressive strength attained 90% of the prescribed design value, ensuring optimal structural integrity and performance.

2.2 Finite Element Model

Fig. 2 presents the FE model of the SG/SF Ramp Bridge. The entire bridge model of the SF/SG Ramp Bridge was established by using the beam element [17] in FE analysis software to evaluate the stress level in the construction process. The model consists of 120 nodes and 110 elements. During construction, the superstructure and the pier are temporarily consolidated, with the 0# block (situated at the bridge pier) fully constrained to support. In addition, the construction of the girder segments was carried out simultaneously on both sides, and the construction period of each segment was about 28 days.

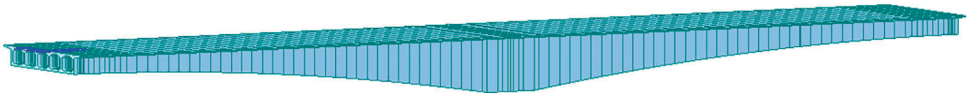

Figure 2: The FE model of the SF/SG Ramp Bridge

Fig. 3 presents the schematic diagram illustrating the deflection and theoretical camber of the bridge derived from the results of the FE model. The maximum deflection caused by the permanent load is

observed at the connection of the right cast-in-place section, measuring 112.5 mm. The deflection resulting from a half-live load is nearly symmetrical along the pier axis, with the right side experiencing a slightly larger deflection, reaching a maximum of 3.9 mm. This discrepancy arises because, despite the left and right ends being symmetrical in the main view, the top view (see Fig. 1) reveals that the right side is wider than the left, creating an asymmetry. Consequently, the effects of self-weight differ between the two sides. As a result, the theoretical pre-camber on the right side is higher than on the left, with the maximum pre-camber occurring on the right side.

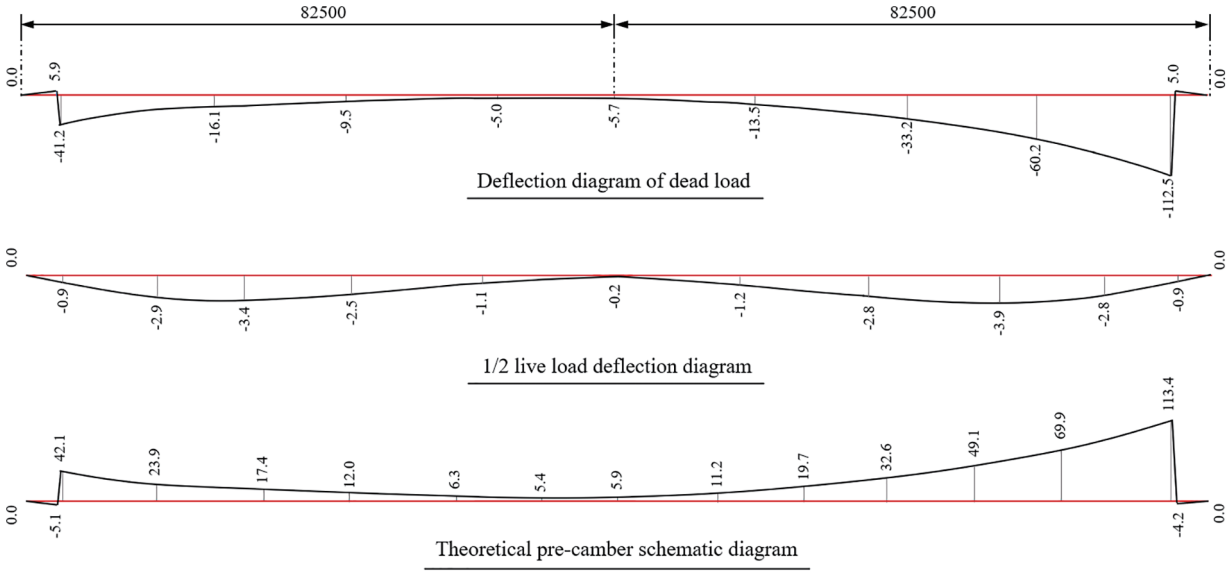

Figure 3: Schematic diagram of deflection and theoretical pre-camber of the bridge (unit: mm)

3 Establishment of Construction Monitoring and Control System

3.1 The Significance of Construction Monitoring

The PC continuous girder bridge was constructed using cast-in-place methods with full-tower support and segmental casting. The construction process consists of multiple cycles, each of which involves the erection of formwork, pouring of concrete, and prestressing of steel strands. The prestressing tension was implemented in all three principal directions, namely longitudinal, transverse, and vertical. The bridge's steel strands arrangement encompassed the top slab, web, and bottom slab of the box girder. Consequently, deviations from the design displacement values can occur at each stage due to changes in the construction process. Suppose these deviations are not promptly identified and corrected through effective construction control. In that case, they can result in the girder line shape failing to meet design specifications or compromising structural integrity during construction. To ensure the vertical displacement of the main girder remains within permissible limits and the bridge deck aligns properly upon completion, it is crucial to establish clear guidelines for controlling the main girder's deflection, stress, and other construction parameters. Effective management and control of these parameters during construction are essential to ensure the bridge's safety and that the main girder conforms to the design requirements after construction is completed.

3.2 Construction Monitoring and Control System

A comprehensive construction monitoring and control system based on multi-party coordination has been established to facilitate the smooth progression of the main girder construction stage, as depicted in

Fig. 4. This system integrates contributions from both the bridge design and construction teams, ensuring seamless collaboration and standardize the operation process of the construction personnel.

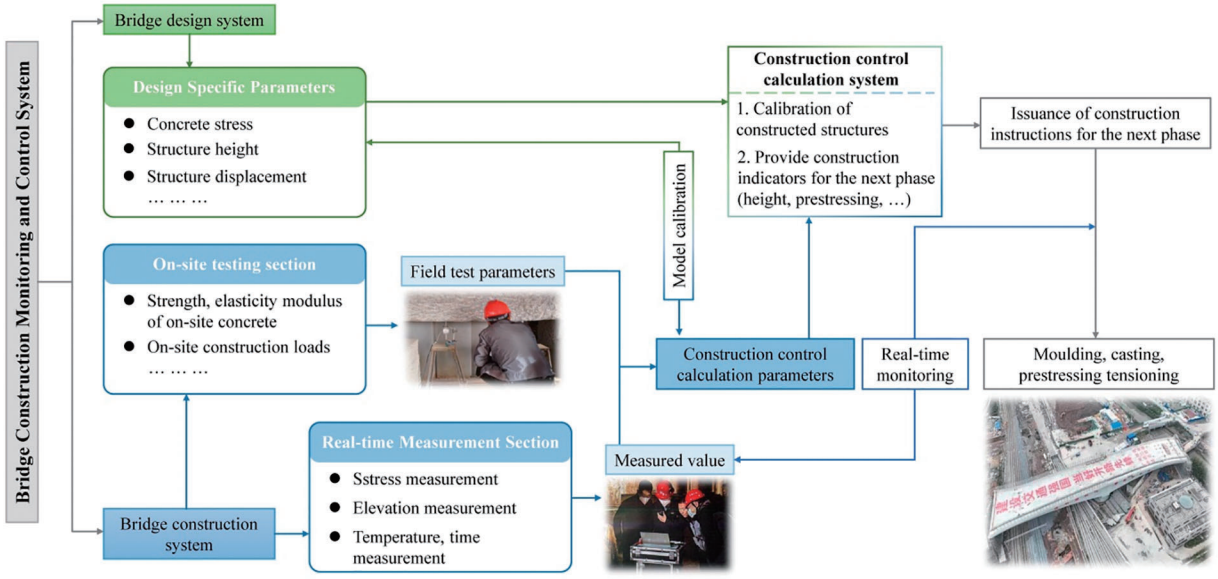

Figure 4: The construction monitoring and control system of the SF/SG Ramp Bridge

The design system is responsible for providing the theoretical design indices of the bridge before construction begins. The construction system comprises two main components: the Real-Time Measurement Section (RMS) and the On-Site Testing Section (OTS). The RMS monitors the geometric and mechanical changes of the structure in real-time during the construction process. The OTS tests the actual mechanical properties of the materials used and assesses the bridge loads. Together, these components supply essential parameters for construction control calculations. By integrating these parameters with the design indices, the construction control calculation system can offer reliable metrics and predictive adjustments for subsequent construction steps, ensuring the bridge is constructed according to design specifications and safety standards. In the construction process, the implementation of the subsequent step in the construction must be carried out subsequent to the completion of the preceding step and its fulfillment of the requisite standards. This is to preclude the amplification of errors that may have arisen in the preceding step from being compounded in the subsequent step.

4 Structural Monitoring and Analysis

4.1 Monitoring Control Projects

4.1.1 Bridge Alignment Monitoring

During the casting process of the main girder, the elevation control of the girder section formwork is crucial for ensuring that the girder's line shape is smooth and conforms to design requirements. Therefore, it is necessary to calibrate and control the height of the formwork before casting. However, the formwork elevation during actual construction often differs from the designed bridge elevation, necessitating the incorporation of a certain pre-camber to offset deformation caused by various factors, such as temporary loads and bracket deformation [18,19]. The specific calculation method for this pre-camber is shown in Eq. (1). The value for bracket deformation is determined through a pre-compression test, which is accounted for in the construction process.

$$H_{lmi} = H_{sji} + \sum H_{1i} + \sum H_{2i} + H_{3i} + H_{4i} + H_{5i} + H_{zj} \tag{1}$$

where, H_{lmi}–Stage i formwork elevation, H_{sji}–Stage i design elevation, ΣH_{1i}–Sum of deflections generated by the self-weight of the girder section at stage i during this and subsequent construction stages, ΣH_{2i}–Deflection caused by prestressing tensioning at this stage and prestressing tensioning at subsequent construction stages at stage i, H_{3i}–Deflection due to concrete shrinkage and creep at stage i, H_{4i}–Deflections due to temporary construction loads during the stage i, H_{5i}–Take the 1/2 value of the deflection caused by the service load during the stage i, H_{zj}–Bracket deformation value.

After each construction cycle, comprehensive measurements must be conducted to analyze the discrepancies between the actual construction outcomes and the expected targets. This analysis allows for timely adjustments to correct any errors that have already occurred. The forecast for the subsequent construction cycle can only proceed once the required accuracy is achieved. According to the Chinese code "Inspection and evaluation quality standard for highway engineering (JTG F80/1-2017)" [20], the deviation between the finished bridge's alignment and the designed alignment must be within ±20 mm, with a merging error within 20 mm.

Fig. 5 illustrates the elevation measurement point arrangement of the SG/SF Ramp Bridge. Fig. 5a displays the longitudinal alignment monitoring points along the entire bridge, using the bridge deck at the centerline of the abutment as the reference point, with monitoring extending to both sides. Fig. 5b shows the transverse measurement points of the bridge section. The longitudinal and transverse elevations of the bridge were monitored to ensure that the structure conforms to the designed height. All measurements were subject to comprehensive monitoring via the use of total stations.

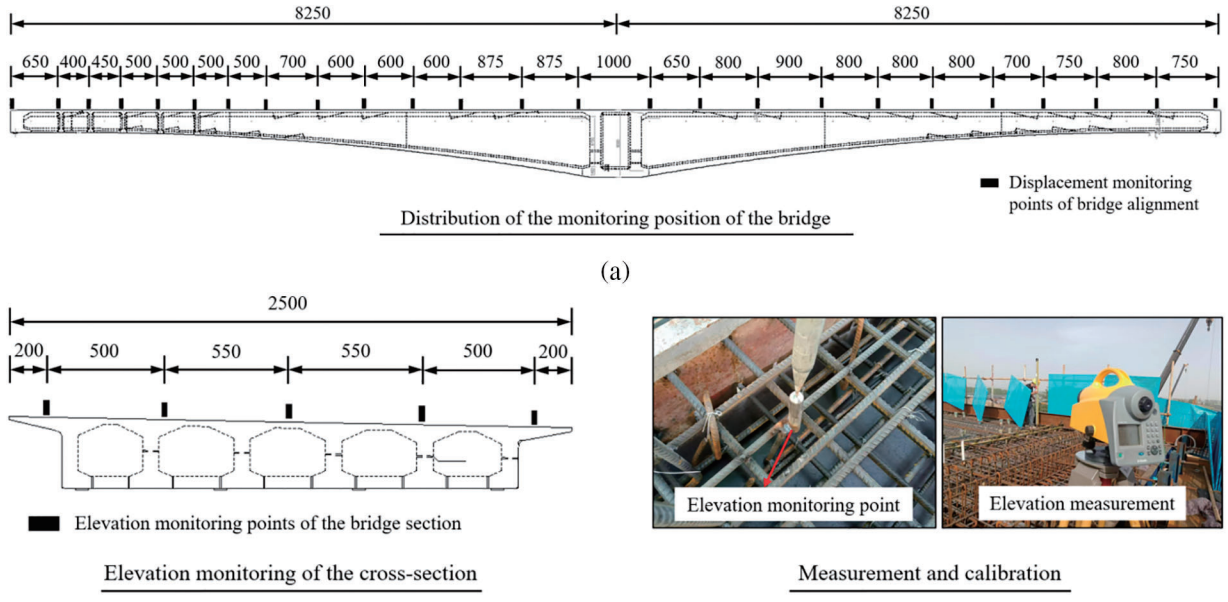

Figure 5: Elevation measuring point arrangement of the SG/SF Ramp Bridge: (a) Full-bridge longitudinal linear monitoring points; (b) Transverse measuring point of the bridge section (unit: cm)

4.1.2 Construction Stress Monitoring

The construction period of bridges is often lengthy, necessitating continuous stress monitoring throughout the entire construction cycle. This monitoring is indispensable for assessing whether the structural and mechanical parameters meet predetermined criteria and providing timely data to guide subsequent construction phases. In this project, stress monitoring was conducted using steel string strain

gauges known for their robust strain accumulation capabilities and resilience against interference, making them ideal for long-term observation.

Fig. 6 illustrates the key cross-sections and instrument arrangement for stress monitoring across the bridge. Six locations were selected as stress monitoring cross-sections, symmetrically distributed on both sides of the bridge abutment. The ZX-216AT embedded temperature-type vibrating wire strain gauges were used, which allows for automatic correction of stress monitoring results based on the internal temperature of the concrete. Following their installation and testing for compliance, all sensors were calibrated.

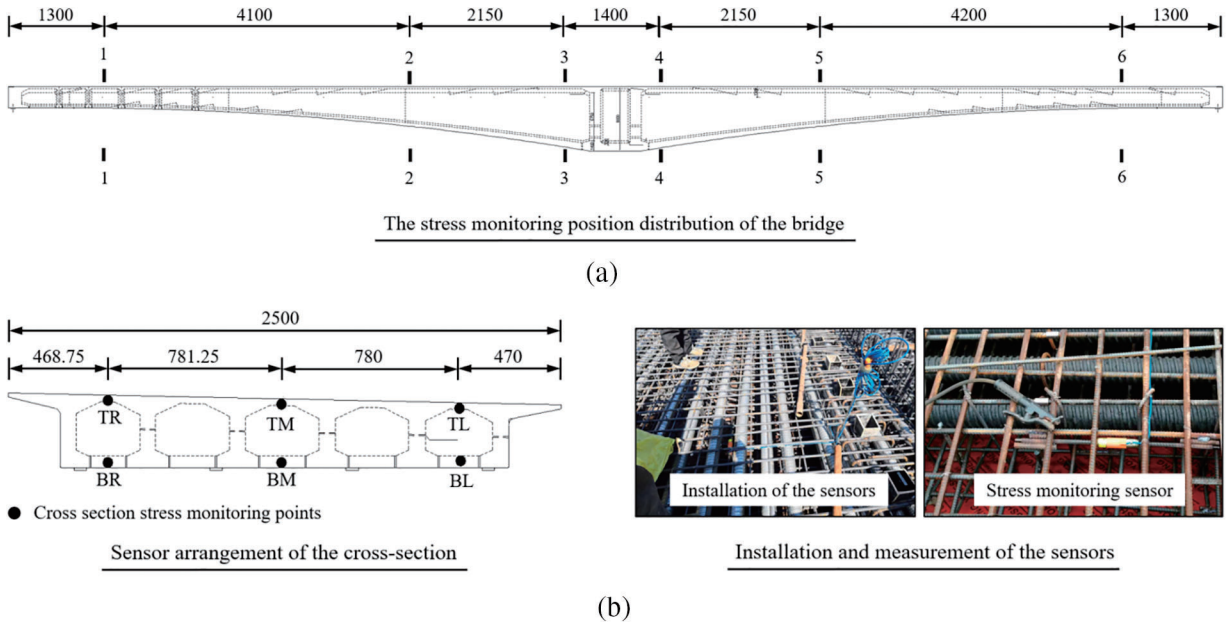

Figure 6: The arrangement of stress measuring points of SG/SF Ramp Bridge: (a) Monitoring section of the whole bridge; (b) The bridge section monitoring points (unit: cm)

Hyperstatic structures constructed using reinforced concrete are subject to secondary internal forces and stress redistribution between reinforcement and concrete due to the shrinkage and creep of concrete. Consequently, the stress changes detected by sensors must account for the effects of concrete shrinkage and creep [21–24]. During normal bridge operation, when the elastic stress is less than 40% of the elastic limit, it is reasonable to assume that the creep strain is proportional to the initial elastic strain [25]. This allows the application of the iterative principle to the elastic strains generated by various factors in the elastic phase. For concrete with an initial stress $\sigma(\tau_0)$ applied at time τ_0, and subsequent stress increments $\Delta\sigma(\tau_i)$ applied incrementally at different times τ_i (i = 1, 2, ..., n), the total strain, including shrinkage strain, at any subsequent time t can be expressed as Eq. (2) [24]:

$$\varepsilon(t,\tau_0) = \frac{\sigma(\tau_0)}{E(\tau_0)}[1+\phi(t,\tau_0)] + \sum_{i=1}^{n}\frac{\Delta\sigma(\tau_i)}{E(\tau_i)}[1+\phi(t,\tau_i)] + \varepsilon_s(t,\tau_0) \tag{2}$$

where, (τ_0)−Initial stress applied at the moment τ_0; $E(\tau)$−Modulus of elasticity of concrete at age τ; $\varepsilon_s(t, \tau_0)$ −The shrinkage strain of concrete at the moment t is calculated using the Chinese code [26]; $\varphi(t, \tau_0)$−The coefficient of creep, which was calculated using Chinese code [26].

Let the data be collected immediately after each applied stress increment $\Delta(\tau_i)$, i.e., the observation moment $t_i = \tau_i$, then the expressions for the moments τ_0, τ_1:

$$\sigma(\tau_0) = \frac{[\varepsilon(\tau_0, \tau_0) - \varepsilon_s(\tau_0, \tau_0)]}{[1 + \phi(\tau_0, \tau_0)]} E(\tau_0) \tag{3}$$

$$\Delta\sigma(\tau_1) = \frac{\left\{[\varepsilon(\tau_1, \tau_0) - \varepsilon_s(\tau_1, \tau_0)] - \frac{\sigma(\tau_0)}{E(\tau_0)}\right\}}{[1 + \phi(\tau_1, \tau_1)]} E(\tau_1) \tag{4}$$

where, $\varepsilon(\tau_0, \tau_0)$–Strain observation needs to be subtracted from the initial measurement value of the sensor.

Similarly, the stress expression at the moment τ_i can be derived as:

$$\Delta\sigma(\tau_i) = \left\{\varepsilon(\tau_i, \tau_0) - \varepsilon_s(\tau_i, \tau_0) - \frac{\sigma(\tau_0)}{E(\tau_0)}[1 + \varphi(\tau_i, \tau_0)] - \sum\nolimits_{n=1}^{i-1} \frac{\Delta\sigma(\tau_n)}{E(\tau_n)}[1 + \varphi(\tau_i, \tau_n)]\right\} \cdot \frac{E(\tau_i)}{[1 + \varphi(\tau_i, \tau_i)]} \tag{5}$$

Therefore, at the moment of τ_i, the elastic strain of concrete at the measuring point after deducting the shrinkage and creep effects is:

$$\varepsilon(\tau_i, \tau_0)_t = \frac{\sigma(\tau_0)}{E(\tau_0)} + \sum\nolimits_{i=1}^{n} \frac{\Delta\sigma(\tau_i)}{E(\tau_i)} \tag{6}$$

Additionally, since the heat of hydration at the initial setting has not yet caused a rise in concrete temperature, and concrete contraction has not occurred, the strain gauges monitoring value at this initial setting moment was generally chosen to set the initial stress value. This approach ensures that the strain gauges do not record stress growth before the concrete is subjected to any load.

4.2 Monitoring Results and Discussion

4.2.1 Bridge Alignment Monitoring

Fig. 7 illustrates the final girder section casting and the vertical displacement of the entire bridge following prestressing tensioning. The overall displacement after concrete pouring indicates a higher left side and lower right side, potentially due to the inherent asymmetry of the bridge and the varying weights of the concrete in the poured sections. Despite this, the maximum difference between the measured and calculated displacement is only 6.23 mm, demonstrating that the overall displacement aligns well with the calculated results. Fig. 7b depicts the displacement of the bridge after the final stage of prestressing tensioning, marking the near completion of the overall construction process. On the right side, a significant displacement occurs approximately 70 m from the beam centerline, attributed to changes in the local force distribution caused by the final stage of prestressing tensioning. The maximum difference in this case is only 6.39 mm, indicating that the structural displacement is well controlled, with a maximum error of under 10 mm.

Fig. 8 compares the bridge's contours after the final construction phase is completed. The overall pre-arch lineal shape after the completion of concrete placement and after the completion of prestressing tension is the same. This indicates that the structural displacements induced by the completion of the final stage of prestressing tension are accumulated in the different sections, resulting in the structure continuing to increase in displacement error. The structure arch will be further increased due to the action of the reverse moment after prestressing tension. Benefiting from the monitoring and control of all steps, after all construction phases were completed, the maximum difference between the measured line shape and the ideal line shape was 17.7 mm, which was less than the limit of ±20 mm specified in the specification.

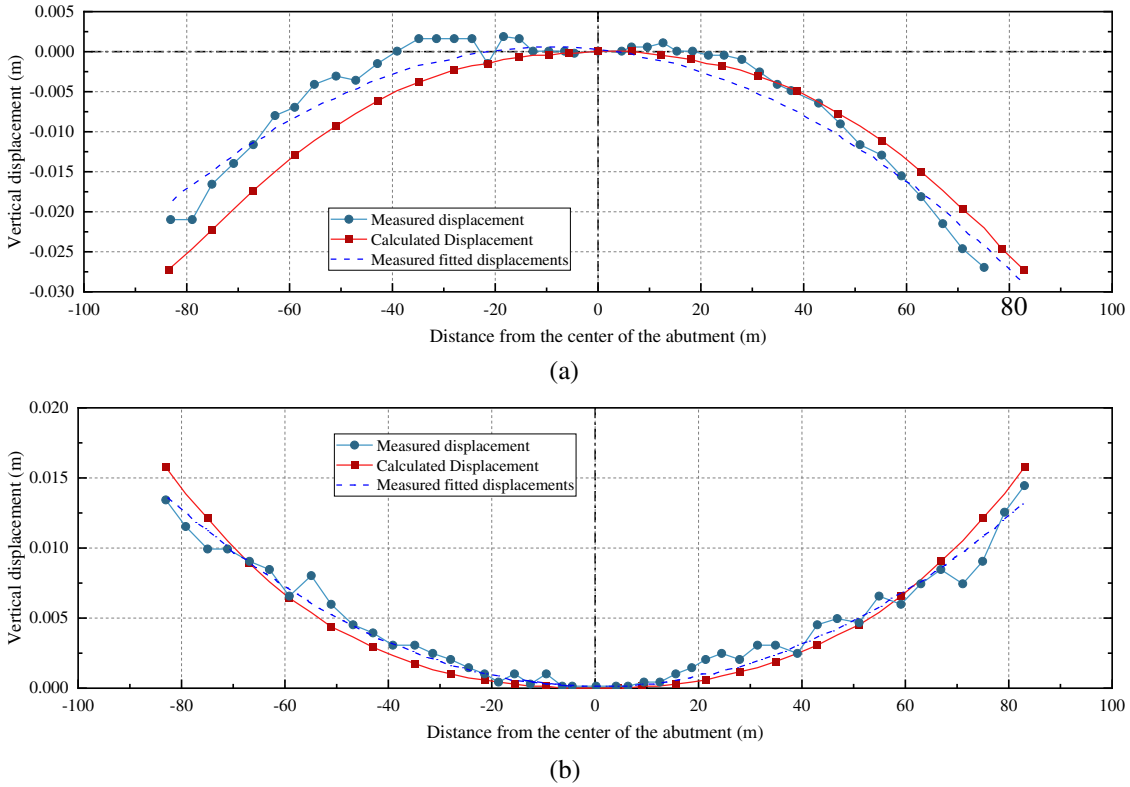

Figure 7: Comparison of displacements during the main girder construction stage: (a) Displacement after the last stage of concrete pouring; (b) Displacement after the last stage of prestressing tensioning

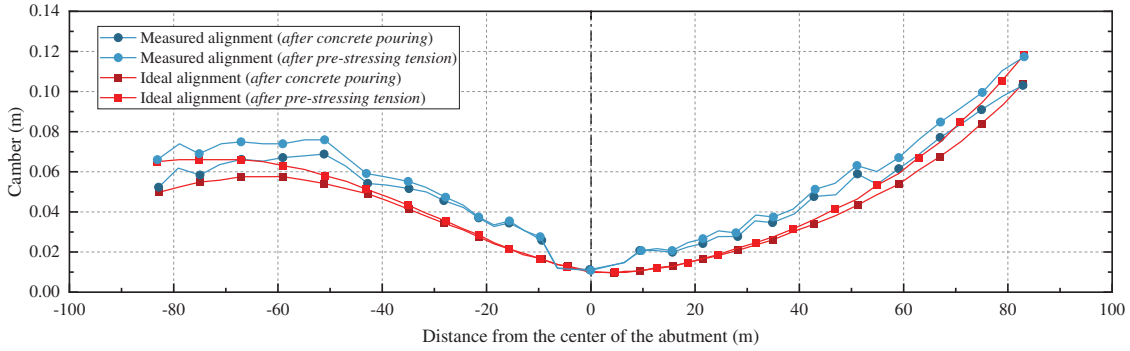

Figure 8: Bridge alignment in the construction stage

Fig. 9 illustrates the bridge alignment under Phase II constant loads after the bridge was paved. At this phase (Phase II), the bridge has been merged, and the deck facilities have been installed. The colored area in the Fig. 9 indicates the regional alignment of the prototype bridge, showing that the overall alignment meets expectations, with a maximum error of 6 mm, which conforms to the specification requirements.

Monitoring results of the bridge alignment demonstrate that throughout the construction process, the bridge alignment varies across different construction phases. Therefore, it is essential to monitor the alignment at each phase and make timely corrections and adjustments based on the measurement results in subsequent construction phases to prevent the accumulation of errors.

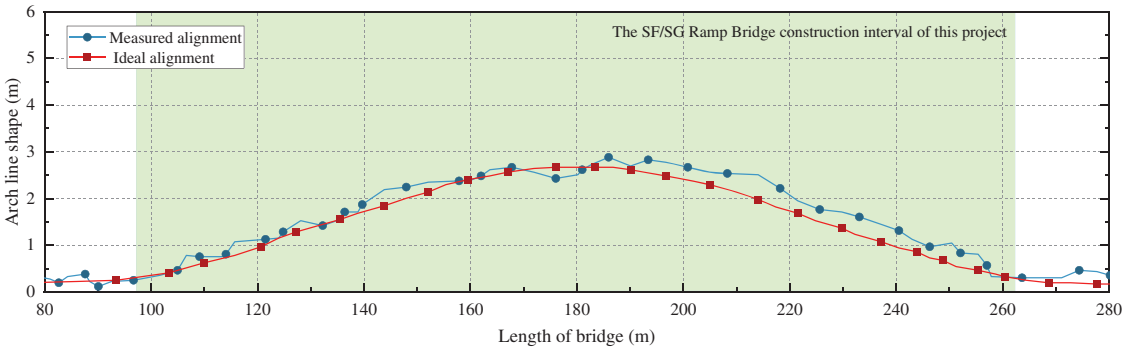

Figure 9: Comparison of the entire bridge alignment after Phase II constant load paving

4.2.2 Structural Stress Monitoring

According to the monitoring above program, stress monitoring of the structure accompanied the entire bridge construction process, with real-time feedback provided to inform subsequent construction steps. The stress monitoring results and calculated stresses for the girders of the bridges in this project, upon completion of construction, are presented in Table 1. Given the extensive volume of monitoring data, only the data for the midpoints of the top slab and bottom slab in the six control sections are shown here. The results obtained from the sensors were used to calculate the stresses in the concrete structure by deducting the shrinkage and creep produced by the concrete.

Table 1: Cross-section stress measured value and calculated value

Section location		Initialization value (MPa)	Final measured value (MPa)	Stress increment with shrinkage and creep (MPa)	Stress increment (MPa)	Concrete stress (MPa)
Section 1-1	TM	36.30	87.30	51.00	37.23	6.78
	BM	85.00	137.00	52.00	38.23	6.96
Section 2-2	TM	52.30	109.30	57.00	41.25	7.51
	BM	39.90	119.30	79.40	57.29	10.44
Section 3-3	TM	93.20	147.20	54.00	39.47	7.19
	BM	32.90	93.60	60.70	44.07	8.03
Section 4-4	TM	68.30	124.20	55.90	40.77	7.43
	BM	25.80	82.90	57.10	40.80	7.43
Section 5-5	TM	35.70	91.90	56.20	41.53	7.56
	BM	58.80	133.70	74.90	54.99	10.02
Section 6-6	TM	39.00	89.00	50.00	36.07	6.57
	BM	91.00	143.10	52.10	37.73	6.87

Note: The positive stress value in the table indicates compression and the negative value indicates tension.

Fig. 10 compares the concrete stresses in the top and bottom slabs of the bridge with the theoretical values. The stresses in the top slab tend to be higher in the middle and lower on both sides. The

difference from the theoretical values increases closer to the middle due to the increased pre-compressive stresses in the middle of the girder segments that are poured on both sides after prestressing tensioning. The measured concrete stresses in the middle of the bottom slab, as shown in Fig. 10b, are symmetrically distributed at the symmetrical locations of the bridge, and the theoretical values are generally close to the measured values. The higher concrete stresses on both sides may result from the significant increase in pre-compressive stresses after tensioning the prestressing bundles in the bottom slab of the last cast girder section. Stress monitoring will continue after the bridge has completed the second phase of constant load placement, such as deck pavement loading. All monitored stresses in the project comply with the Chinese code [27] requirements of a limited value of $\sigma_{cc}^{t} \leq 0.70 f_{ck}' = 24.85$ MPa (Where, σ_{cc}^{t} represents concrete compressive stress; f_{ck}' represents the concrete standard value of axial compressive strength) for concrete normal compressive stress at the edge of the cross-section of prestressed concrete bending members under transient conditions, such as construction loads from prestressing force and the member's weight, ensuring safe construction and building integrity.

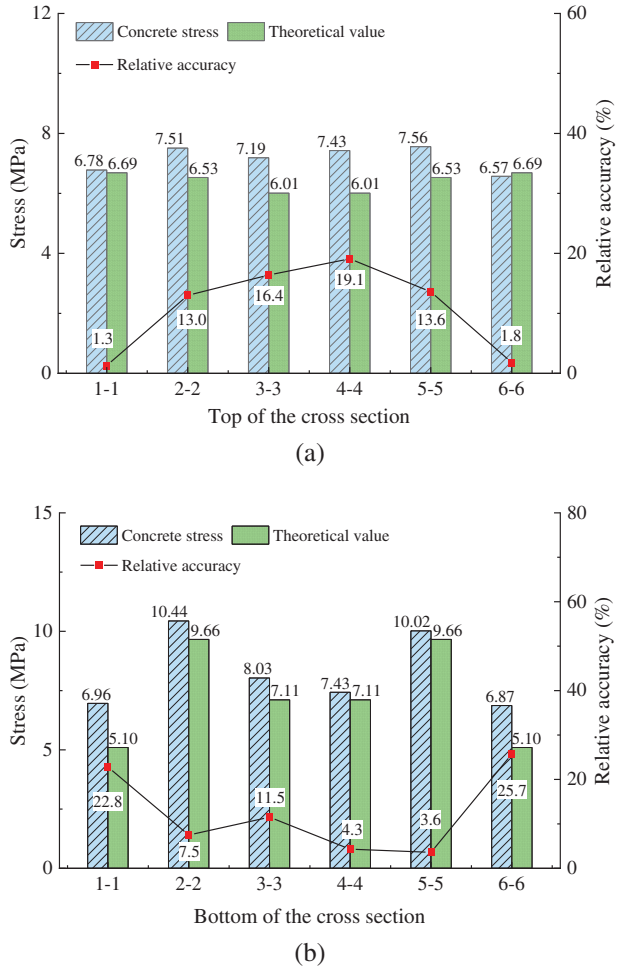

Figure 10: Comparison of the measured value and theoretical value: (a) The middle of the top of the cross-section; (b) The middle of the bottom of the cross-section

5 Conclusions

This paper employs the SF/SG Ramp Bridge in China as a case study for engineering analysis. During the bridge's construction, a comprehensive monitoring program was implemented to assess the alignment and stress levels. The resulting data was analyzed to identify key insights, which are presented below:

(1) Construction monitoring is crucial to the bridge construction process. This paper proposes a construction monitoring feedback system to guide the construction process. The system clarifies the monitoring content, including field testing, and integrates it with theoretical analysis to inform subsequent construction phases. The practical application demonstrates that this construction monitoring feedback system ensures the bridge construction is conducted safely and meets the final design requirements.

(2) Linear monitoring of the bridge was conducted, and the results indicated that the bridge's alignment conformed to the design requirements upon completion of construction. The maximum difference between the vertical displacement and the ideal state after prestressing tensioning was 6.39 mm, and the maximum difference between the pre-arching degree and the ideal state was 17.7 mm. These differences fall within the specified limits.

(3) Concrete stresses after the completion of bridge construction were monitored using embedded sensors. The monitored concrete stresses met the code's limit requirements, closely matched the theoretical values, and exhibited a symmetrical trend along the centerline. The final stage of prestressing tensioning increased the compressive stresses in the concrete top slab and the bottom slabs on both sides of the bridge.

Acknowledgement: The authors express their sincere gratitude for the help provided by Lanzhou Jiaotong University in monitoring the strains of the prototype bridge.

Funding Statement: The Guangdong Basic and Applied Basic Research Foundation (Grant # 2023A1515010535).

Author Contributions: The authors confirm contribution to the paper as follows: Writing—original draft preparation, Data curation, Conceptualization, Yi Wang; Writing—original draft preparation, Investigation, Bing Wang; Methodology, Validation, Changwen Li; Resources, Data curation, Feng Zheng; Conceptualization, Validation, Yong Liu; Funding acquisition, Supervision, Visualization Preparation, Writing—review & editing, Shaohua He. All authors reviewed the results and approved the final version of the manuscript.

Availability of Data and Materials: The data that support the findings of this study are available from the corresponding author upon reasonable request.

Ethics Approval: Not applicable.

Conflicts of Interest: The authors declare no conflicts of interest to report regarding the present study.

References

1. Yu L, Qiao TZ, Bao LS, Zhu GS. Prestressed concrete continuous girder bridge reinforcement simulation analysis and carrying capacity assessment. Adv Mater Res. 2012;594:1516–21. doi:10.4028/www.scientific.net/AMR.594-597.1516.
2. Yang XM, Wang ZW, Zheng X, Guan ZX, Yang DH, Yi TH. Structural health monitoring of long-span continuous girder bridge: system implementation and data analysis. Int J Struct Stab Dyn. 2024;2550009. doi:10.1142/S0219455425500099.

3. Liu L, Zhang ZW, Ma XP, Yu SS, Lv HW. Comparative study on linear shape of cantilever construction of railway continuous bridge with different spans. J China Foreign Highway. 2019;39(5):93–7 (In Chinese). doi:10.14048/j.issn.1671-2579.2019.05.018.
4. Zhao SJ, Tang XB, Ren WX. The statistical characteristics analysis of bridge accidents and prevention principle of security risk. J Railway Eng Soc. 2017;5:59–64 (In Chinese). doi:10.3969/j.issn.1006-2106.2017.05.011.
5. Latupeirissa JE, Wong ILK, Tiyow HC. Causes of work accidents and its impact on the road and bridge construction projects. IOP Conf Series: Earth Environ Sci. 2021;907(1):012–23. doi:10.1088/1755-1315/907/1/012023.
6. Asanka WA, Ranasinghe M. Study on the impact of accidents on construction projects. In: 6th International Conference on Structural Engineering and Construction Management, 2015; Kandy, Sri Lanka; vol. 4, p. 58–67.
7. Ovchinnikov II, Maystrenko IY, Ovchinnikov IG, Uspanov AM. Accidents and destruction of bridge structures, analysis of their causes. Russ J Transp Eng. 2017;4(4):2. doi:10.15862/13TS417.
8. Dergunov SA, Satyukov AB, Spirina AY, Serikov SV. Accidents of bridge structures and their causes. Bull KSUCTA. 2019;2(64):289–94. doi:10.35803/1694-5298.2019.2.289-294.
9. Ouyang J, Wang HJ, Wu LX, Zhang KX, Xue X. Construction monitoring and analysis of low mountain ridge tunnel. Arch Civil Eng. 2024:573–87. doi:10.24425/ace.2024.148929.
10. Wang J, Li G, Lan C, Guo N. Experiment of the monitoring prestress loss of prestressed concrete beams with damages under static loading. Arch Civil Eng. 2023:437–51. doi:10.24425/ace.2023.144182.
11. Zasukhin I, Ivanov A, Kuzmenkov P, Polyakov S, Chaplin I. Features of monitoring the stress-strain state of structures during the construction of bridge crossings. Int Scientific Siberian Transport Forum. 2021;403(1):72–81. doi:10.1007/978-3-030-96383-5_9.
12. Li FY, Wu PF, Yan XF. Analysis and monitoring on jacking construction of continuous box girder bridge. Comput Concr. 2015;16(1):49–65. doi:10.12989/cac.2015.16.1.049.
13. Yin T, Zhang W, Zhao YB, Sun XL. Construction monitoring technology research on large-span V structure tied arch bridge. Appl Mech Mater. 2013;351–352:1240–3. doi:10.4028/www.scientific.net/AMM.351-352.1240.
14. Inaudi D, Casanova N, Kronenberg P, Vurpillot S. Railway bridge monitoring during construction and sliding. In: SPIE Conference on Smart Structures and Materials, 1997; San Diego, CA, USA; vol. 3043, p. 58–64. doi:10.1117/12.274655.
15. Zhang KX, Shen XY, Bao LS, Liu H. Process monitoring and terminal verification of cable-stayed bridges with corrugated steel webs under construction. Struct Durability Health Monitor. 2023;17(2):131–58. doi:10.32604/sdhm.2023.023431.
16. Idriss RL. Monitoring of a smart bridge with embedded sensors during manufacturing, construction and service. In: Third International Conference on Health Monitoring, 2001; Stanford, CA, USA.
17. Wang SH, Li XJ. Vibration characteristics analysis and structure optimization of catenary portal structure on four-wire bridge. Struct Durability Health Monitor. 2022;16(4):361–82. doi:10.32604/sdhm.2022.023851.
18. Mosallam K, Chen WF. Design considerations for formwork in multistorey concrete buildings. Eng Struct. 1990;12(3):163–72. doi:10.1016/0141-0296(90)90003-B.
19. Wang H. Analysis of construction technology of cast-in-place box girder in road and bridge construction. Sichuan Build Mater. 2024;50(5):139–41 (In Chinese).
20. MOHURD (Ministry of Housing and Urban-Rural Development of the People's Republic of China). JTG F80/1-2017: inspection and evaluation quality standard for highway engineering. Beijing: China Architecture & Building Press; 2017.
21. Wang SQ, Fu CC. Simplification of creep and shrinkage analysis of segmental bridges. J Bridge Eng. 2015;20(8):B6014001. doi:10.1061/(ASCE)BE.1943-5592.0000728.
22. He SH, Lv BT, Huang X, Zuo LQ, Zhou DF. Cracking performance in the hogging moment region of HSS-UHPC continuous composite girder bridges. Structures. 2024;61(4):106081. doi:10.1016/j.istruc.2024.106081.
23. He SH, Huang X, Zou LQ, Zheng C, Xin HH, Liang JH. Performance assessment of channel beam bridges with hollow track bed decks. Structures. 2024;61(2):105988. doi:10.1016/j.istruc.2024.105988.

24. Zou DJ, Liu TJ, Teng J, Du CC, Li B. Influence of creep and drying shrinkage of reinforced concrete shear walls on the axial shortening of high-rise buildings. Constr Build Mater. 2014;55(2):46–56. doi:10.1016/j.conbuildmat.2014.01.034.
25. American Concrete Institute (ACI) Committee 209. Prediction of creep, shrinkage and temperature effects in concrete structures. ACI 209R-92: designing for effects of creep, shrinkage and temperature. Detroit. 2008;51–93.
26. Gong JW. Linear monitoring technology of long-span continuous girder bridge of high-speed railway. China Collect Econ. 2011;30:176–80 (In Chinese). doi:10.3969/j.issn.1008-1283.2011.30.102.
27. MOHURD (Ministry of Housing and Urban-Rural Development of the People's Republic of China). JTG 3362–2018: specifications for design of highway reinforced concrete and prestressed concrete bridges and culverts. Beijing: China Architecture & Building Press; 2018.